HAL open science

# Extraction of homogeneous lignin oligomers by ozonation of Miscanthus giganteus and vine shoots in a pilot scale reactor

M. Ebrahimi, V. Acha, L. Hoang, A. Martínez-Abad, A. López-Rubio, L. Rhazi, Thierry Aussenac

**To cite this version:**

M. Ebrahimi, V. Acha, L. Hoang, A. Martínez-Abad, A. López-Rubio, et al.. Extraction of homogeneous lignin oligomers by ozonation of Miscanthus giganteus and vine shoots in a pilot scale reactor. Bioresource Technology, 2024, 402, pp.130804. ⟨10.1016/j.biortech.2024.130804⟩. ⟨hal-04573413⟩

**HAL Id: hal-04573413**

**https://hal.science/hal-04573413v1**

Submitted on 16 May 2024

**HAL** is a multi-disciplinary open access archive for the deposit and dissemination of scientific research documents, whether they are published or not. The documents may come from teaching and research institutions in France or abroad, or from public or private research centers.

L'archive ouverte pluridisciplinaire **HAL**, est destinée au dépôt et à la diffusion de documents scientifiques de niveau recherche, publiés ou non, émanant des établissements d'enseignement et de recherche français ou étrangers, des laboratoires publics ou privés.

Autorisation HAL

HAL Authorization

Bioresource Technology 402 (2024) 130804

Contents lists available at ScienceDirect

Bioresource Technology

journal homepage: www.elsevier.com/locate/biortech

Case Study

# Extraction of homogeneous lignin oligomers by ozonation of *Miscanthus giganteus* and vine shoots in a pilot scale reactor

M. Ebrahimi [a,b], V. Acha [a], L. Hoang [a], A. Martínez-Abad [b], A. López-Rubio [b], L. Rhazi [a], T. Aussenac [a,*]

[a] *Institut Polytechnique UniLaSalle, Université d'Artois, ULR 7519, 19 rue Pierre Waguet, BP 30313, 60026 Beauvais Cédex, France*
[b] *Food Safety and Preservation Department, IATA-CSIC, Avda. Agustín Escardino 7, 46980 Paterna, Valencia, Spain*

## HIGHLIGHTS

- An ozonation 200 L pilot scale reactor was used to extract lignin from biomass.
- Homogeneous lignin oligomers were extracted by ozonation.
- Lignin extracted fractions from vine shoots had higher molecular weight.
- *Miscanthus giganteus* released higher quantity of phenolic monomers after ozonation.
- Thermally stable lignin fractions were extracted from both biomasses by ozonation.

## GRAPHICAL ABSTRACT

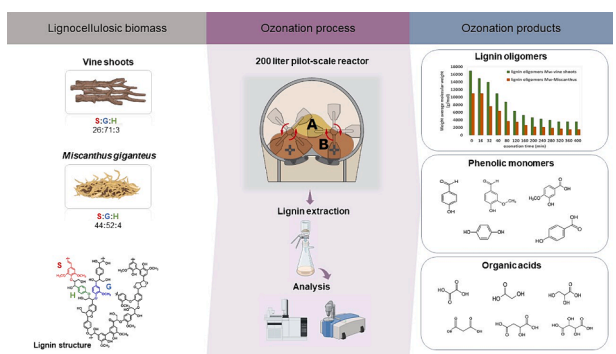


## ARTICLE INFO

*Keywords:*
Ozonation
Lignin oligomers
Extraction
*Miscanthus giganteus*
Vine shoots

## ABSTRACT

Lignin, a complex phenolic polymer crucial for plant structure, is mostly used as fuel but it can be harnessed for environmentally friendly applications. This article explores ozonation as a green method for lignin extraction from lignocellulosic biomass, aiming to uncover the benefits of the extracted lignin. A pilot-scale ozonation reactor was employed to extract lignin from *Miscanthus giganteus* (a grass variety) and vine shoots (a woody biomass). The study examined the lignin extraction and modification of the fractions and identified the generation of phenolic and organic acids. About 48 % of lignin was successfully extracted from both biomass types. Phenolic monomers were produced, vine shoots yielding fewer monomers than *Miscanthus giganteus*. Ozonation generated homogeneous lignin oligomers, although their molecular weight decreased during ozonation, with vine shoot oligomers exhibiting greater resistance to ozone. Extracted fractions were stable at 200 °C, despite the low molecular weight, outlining the potential of these phenolic fractions.

* Corresponding author.
*E-mail address:* thierry.aussenac@unilasalle.fr (T. Aussenac).

https://doi.org/10.1016/j.biortech.2024.130804
Received 28 February 2024; Received in revised form 30 April 2024; Accepted 5 May 2024
Available online 6 May 2024
0960-8524/© 2024 The Author(s). Published by Elsevier Ltd. This is an open access article under the CC BY license (http://creativecommons.org/licenses/by/4.0/).

## 1. Introduction

Given the depletion of fossil fuels and growing environmental challenges, the need to develop renewable green resources has become urgent (Zhang et al., 2023). Lignocellulosic biomass is an abundant renewable resource that can provide a sustainable substitute for energy and chemicals (Wang et al., 2023). Lignin is one of the three main biopolymeric fragments, along with cellulose and hemicelluloses found in lignocellulosic biomass; despite its significant quantities in biomass (Danby et al., 2018), lignin is an underestimated constituent as it is not truly valorised due to its complex structure (Rajesh Banu et al., 2019).

Lignin has a three-dimensional structure comprised of phenyl propane units: p-hydroxyphenyl (H), guaiacyl (G), and syringyl (S), which serve as the primary building blocks (Barrera-Martínez et al., 2016). Radical coupling of these phenyl propane units results in the formation of different internal unit bonds, including alkyl-aryl-ether bonds such as β-O-4 (45 to 85 %), α-O-4 (~2%), and carbon–carbon bonds such as β-5 (1 to 12 %), β-β (5 to 12 %), and β-1(1 to 12 %) (Du et al., 2022; Zhou et al., 2022). The overall structure and functional group composition of lignin change depending on both the extraction process and the lignin generation process. This results in significant heterogeneity in its structure, presenting various obstacles to its large-scale, widespread industrial applications (Wang et al., 2023).

Currently, a substantial part of technical lignin, 140 million tons per year (around 98 % of total lignin), is used as fuel for the production of heat and electricity in biorefineries (Becker and Wittmann, 2019). Thus, merely 2 % of lignin is efficiently used, leaving a huge potential to be tapped (Du et al., 2022). With the progress of research on biorefining towards the circular economy, lignin is fortunately emerging as a potentially valuable chemical component, opening up new possibilities for its use (Garlapati et al., 2020). Thanks to its rich phenolic composition, lignin mostly serves as a natural antioxidant, antimicrobial agent (Dong et al., 2011), UV absorber (Ariyanta et al., 2023), and finds applications in packaging (Alzagameem et al., 2022), drug delivery (Figueiredo et al., 2017), and cosmetics (Ariyanta et al., 2023).

To achieve the desired lignin-based products, a controlled extraction process is essential to transform lignin into a consistent and uniform structure (Bajwa et al., 2019). Various technologies have been used for lignin extraction from lignocellulosic biomass, including physical, chemical, and biological approaches. Four main industrial lignin extraction processes are sulfite, Kraft, organosolv, and soda processes. Sulfite and Kraft processes, which generate sulfur-containing lignin, emit sulfur dioxide ($SO_2$), and discharge wastewater containing both organic and inorganic pollutants, leading to environmental pollution. On the other hand, the sulfur-free organosolv lignin is produced using an expensive organic solvent with low extraction yield, which is not a good fit for industrial application. Moreover, all these methods require the use of hazardous materials such as acids, alkalis, and/or organic solvents (Capolupo and Faraco, 2016; Maurya et al., 2015). Therefore, an environmentally-friendly and cost-effective method is required to extract lignin without releasing chemical waste into the environment.

Ozonation is one of the most promising and green oxidation processes for lignin extraction with minimal effect on cellulose and hemicellulose content (Travaini et al., 2016b). Ozone is a strong oxidising agent ($E^0 = 2.07$ V, 25 °C) (Rice and Netzer, 1982). It can be easily generated in situ, either from oxygen or dry air, and the technology is well-established and easily scalable. Ozone has a short half-life, so any residual ozone in the system will quickly break down into oxygen, allowing safe ozonation procedures. It is thus a clean procedure that does not require additional separation steps to remove reagents (Figueirêdo et al., 2020a). Ozone has high reactivity toward compounds having double bonds and functional groups with high electron densities, such as those present in lignin (Shi et al., 2015). Ozonation of lignin was first reported in 1913 (Danby et al., 2018). So far, the ozonation process has been studied with two different goals in lignin-related research. The first goal is the extraction of lignin from biomass to purify cellulose with the aim of producing bioethanol or biohydrogen. The ozonation of wheat bran (Li et al., 2021), wheat straw (Wu et al., 2013), sugarcane bagasse (Travaini et al., 2016a), and corn straw (Shi et al., 2015) have been studied considering this first objective. The second goal is the use of ozone for technical lignin depolymerisation with the aim of lignin valorisation. Technical lignin refers to the native-lignin or proto-lignin derivative obtained as the result of the delignification process. With that in mind, the ozonation of Kraft lignin (Musl et al., 2019), organosolv lignin, ball-milled lignin (Figueirêdo et al., 2020a), and pyrolytic lignin (Figueirêdo et al., 2019) have been reported. However, the structural characterisation of lignin obtained directly from biomass by ozonation has not yet been carried out to determine possible future applications. In this study, two different types of lignocellulosic biomasses, namely *Miscanthus giganteus* and vine shoots, were used to explore the extraction of lignin by ozone treatment, as well as its subsequent characterisation. *Miscanthus giganteus*, recognised as a perennial grass, has an excellent annual biomass yield ranging from 18.7 to 36.8 tons per hectare and contains a high percentage of lignin in its structure, within the range of 15 – 20 %. The main application of this grass nowadays is energy generation through combustion or fast pyrolysis. Its substantial lignin content and high annual yield render it as an interesting candidate for lignin extraction and its higher value-added utilisation (van der Cruijsen et al., 2021). On the other hand, vine shoots, which are abundant pruning agricultural residues derived from the wine industry, have posed challenges in terms of management due to their large volume and low density. Traditionally, they have been either left in vineyards for use as fertilisers or burned, but burning practices raise significant environmental concerns and are subject to strict regulations in many wine-producing countries. Vine shoots have a lignin content from 20 % to 23 %, making them attractive for valorisation purposes as well (Benito-González et al., 2020).

In this paper, the impact of the ozonation process on lignin extraction from *Miscanthus giganteus* and vine shoots was explored using a pilot-scale reactor, along with an examination of the structural modifications taking place during the process. The research involved a study on how specific ozonation parameters, such as pH, ozonation time, or ozone concentration may affect lignin and its potential valorisation from these different biomass sources. The physicochemical properties of the extracted lignin from *Miscanthus giganteus* and vine shoots were characterised by investigating the generation of oligomeric lignin fractions, phenolic acids, and organic acids. A comparison was made between the structural changes in the ozonised and non-ozonised extracted fractions, followed by an investigation into the thermal stability of the extracted fractions. The monitorisation of several ozonation parameters over time was also done in this work, these being very useful information for process optimisation.

## 2. Materials and methods

### 2.1. Biomass preparation

This study used two types of biomass, *Miscanthus giganteus* and vine shoots from the pruning of vine trees, as key components for analysis and evaluation. The *Miscanthus giganteus* sample was supplied by Lamont-Colin Energies (France). It included a mixture of internode components, nodes, blades, and sheaths from the *Miscanthus giganteus* plant. Vine shoots were supplied by Grill O'Bois (France) and only shoots with diameter size between 0.5 – 1.5 cm were used. Prior to the ozonation experiment, the samples underwent grinding and sieving processes to achieve a particle size of < 1 mm and less than < 1.5 mm for *Miscanthus giganteus* and vine shoots, respectively. The prepared samples were then stored at room temperature. Analysis of the samples revealed a moisture content of 6.80 % and 7.04 % for *Miscanthus giganteus* and vine shoots, respectively. Additionally, water activity ($a_w$) was determined using a Novasina water activity meter, resulting in values of 0.534 and 0.405, respectively.

### 2.2. Ozonation process

In order to carry out the ozonation process, a pilot semi-industrial rotary cylindrical reactor with a capacity of 0.200 $m^3$ was used (Fig. 1). Gaseous ozone was generated by a corona electric discharge ozone generator (OZAT CFS14, Ozonia, France) powered by 99.5 % pure oxygen with a dew point of –80 °C (Messer, France). The ozone was introduced into the reactor with an average flow rate of 5 $m^3 \cdot h^{-1}$. To monitor the ozone concentration, measurements were taken at the inlet and outlet of the reactor using a BMT 964 UV ozone analyser (BMT, Germany). The ozone outlet was subjected to thermal destruction at 350 °C. Ozone consumption by biomass was calculated using the following equation (Eq. (1)):

$$Ozoneconsumption\left(g\hat{A}\cdot g^{-1}drybiomass\right) = \frac{\sum\left(C_{O3,in} - C_{O3,out}\right)_{g\hat{A}\cdot m^{-3}} \times gasflowrate_{m^3\hat{A}\cdot h^{-1}} \times time_h}{gdrybiomass} \quad (1)$$

where $C_{O3,in}$ is the ozone concentration at the reactor inlet, and $C_{O3,out}$ is the ozone concentration at the reactor outlet.

For the ozonation experiment of each biomass, the study utilised 20 kg of ground biomass. This biomass was carefully mixed with an equal quantity of water in the reactor. To facilitate the mixing process, pressurised nozzle injectors were used inside the twin-shaft paddle mixer (Stolz®) integrated into the reactor. Then, ozone was introduced into the reactor at a concentration of 140 g $N \cdot m^{-3}$ through a total reaction time of 400 min (N stands for Normal conditions: T = 0 °C, P = 1 atm). To monitor the progress of the ozonation process, ozonised biomass samples were collected from the reactor at specific time intervals, namely 16, 32, 40, 80, 120, 160, 200, 240, 280, 320, 360, and 400 min. Additionally, the temperature of the biomass was monitored throughout the ozonation process. The study also recorded changes in the water activity ($a_w$), moisture content, and pH of the samples, before and during the ozonation process. Preliminary pH measurements were carried out on *Miscanthus giganteus* and vine shoots, yielding values of 6.32 and 6.52, respectively, before starting the ozonation process. After the ozonation process, the collected samples were dried in an oven at 50 °C for 48 h to reduce humidity and facilitate storage before analysis. To establish a referenced comparison, a non-ozonised blank experiment was conducted for both biomasses. In this experiment, pure oxygen (99.5 % purity) from Messer, France, with a dew point of –80 °C, was injected into an equal amount of biomass samples (20 kg). The duration of this experiment was 400 min as well, and samples were collected at the same intervals as those for the ozonised biomass. This experiment served as a control to assess the specific effects of ozonation on the biomass samples.

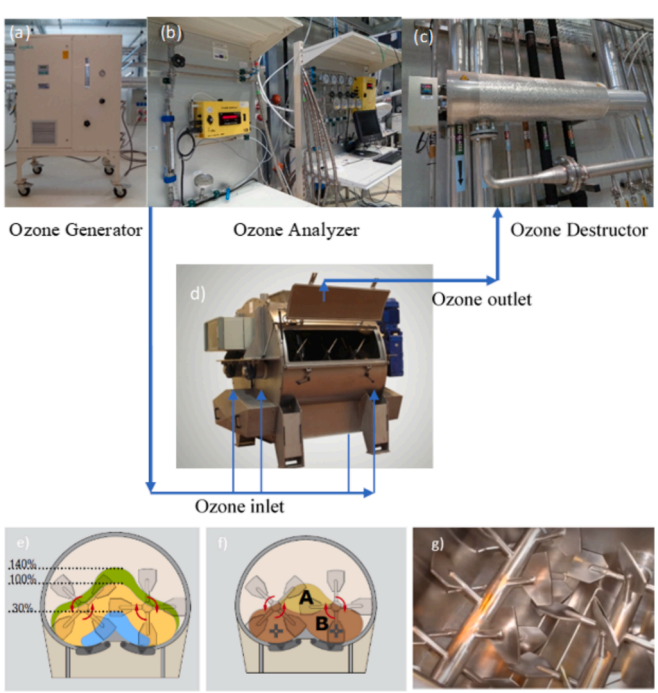


**Fig. 1.** Diagram of ozonation by Twin shaft paddle mixer reactor in the Uni-LaSalle $O_3$ Platform: a) OZAT CFS14 ozone generator; b) BMT ozone analyzer; c) Ozone destroyer; d) Twin shaft paddle mixer reactor (Stolz®), and the characteristic of Twin shaft paddle mixer reactor (capacity from 6L to 10000L): e) percentage of capacity of reactor; f) fluidization and particles movement areas; g) photo of twin shaft paddle.

### 2.3. Obtaining the fractions extracted from Miscanthus giganteus and vine shoots by ozonation in the pilot reactor

4 g of dried ozonised biomass (Miscanthus giganteus and vine shoots) from the pilot reactor was combined with 200 mL of ultra-pure water in 250 mL erlenmeyer flasks. These flasks were subsequently placed in a water bath at 60 °C for 30 min. After the allotted time, the samples were subjected to vacuum filtration using DURAN crucibles to effectively separate the filtrate from the residue. The residue was then carefully dried in an oven maintained at a temperature of 45 °C for 48 h. After that, the filtrate, also referred to as the extracted fraction, was placed in a freezer set to a temperature of –80 °C overnight, and then freeze-dried. The extract yield was calculated using Eq. (2)

$$Extractyield\% = \frac{weightoflyophilisedextract(g)}{weightofinitialdrybiomass(g)} \times 100 \quad (2)$$

### 2.4. Analytical methods

#### 2.4.1. Physical characterisation

The particle size analysis of the ground *Miscanthus giganteus* and vine shoots was performed by laser particle size analysis (Mastersizer 3000, Malvern®). Furthermore, the morphogranulometric distribution of the ground biomass was evaluated using a morphogranulometer (Morphology G3, Malvern®).

#### 2.4.2. Ash content

The analysis of the ash content of untreated biomass was conducted according to the NREL/TP-510–42622 method. To perform this analysis, dry samples were placed in the furnace at 575 °C overnight. The ash content was measured gravimetrically. The analysis was done in triplicate.

#### 2.4.3. Lignin content

The analysis of Klason lignin content of ozonised biomass residue and non-ozonised biomass was carried out using the NREL/TP-510–42618 method. 3 mL of 72 % $H_2SO_4$ was added to 300 mg of extractive-free samples in glass tubes. The tubes were then placed in a water bath at a temperature of 30 °C for one hour, with periodic stirring every 10 min. Then, each acidic solution was diluted to a concentration of 4 % by adding 84 mL of ultra-pure water. The resulting solution was thoroughly mixed and then placed in an autoclave at 121 °C for 1 h. After the autoclave cycle was completed, the hydrolysates were gradually cooled to room temperature. The samples were then subjected to vacuum filtration and the acid-insoluble portion was carefully placed in the oven and dried overnight at 105 °C. The Klason lignin content was measured gravimetrically after drying the remaining solid. The analysis was performed in duplicate.

#### 2.4.4. Holocellulose content

For holocellulose analysis, 2 g of oven-dried sample was placed in a threaded cap glass bottle. 160 mL of ultra-pure water was added to the sample and the bottle was shaken by hand. Then, 20 mL of sodium

chlorite (34 g·L$^{-1}$) and 20 mL of the acetic acid/sodium hydroxide buffer solution (pH 4.9) were added to the sample. After stirring, the bottle was placed in two polyethylene terephthalate (PET) bags, sealed, and placed in a water bath at 70 °C for 2 h. Then, the sample was vacuum filtered under a fume hood, and washed with ultra-pure water until a clear filtrate was obtained. The remaining residue was dried in an oven at 105 °C overnight. The holocellulose content was calculated gravimetrically. The analysis was done in triplicate.

#### 2.4.5. Protein content

The protein content of *Miscanthus giganteus* and vine shoots was analysed by the Dumas combustion method. The Dumas method relies on the combustion of the entire sample at a high temperature in an oxygen-enriched atmosphere. A 100 mg dry sample was used for the measurement. A thermal conductivity detector measured nitrogen gas. The protein content was calculated from nitrogen using a conversion factor of 6.25. The measurements were done in triplicate.

#### 2.4.6. Attenuated total reflection (ATR)-FTIR analysis

ATR-FTIR spectroscopy (Thermo Scientific™, Nicolet™ iN10 MX) was used to examine the structural changes of *Miscanthus giganteus* and vine shoots, and their extracted fractions during the ozonation process. Dry samples were analysed at a spectral range between 400 to 4000 cm$^{-1}$ at a resolution of 4 cm$^{-1}$ for 64 scans. Each ATR-FTIR spectrum is the result of the average of 3 spectral acquisitions.

#### 2.4.7. High-performance size-exclusion chromatography (HPSEC) analysis

The weight average molecular weight ($M_w$), number average molecular weight ($M_n$), and polydispersity index ($M_w/M_n$) of the extracted fractions at different ozonation times were analysed by HPSEC. The SEC configuration was as follows: column, Waters Ultrahydrogel 1000A (column dimensions: 7.8 mm ID × 300 mm); eluent, 0.1 M NaOH (titrated with HCl to pH 12.0); flow rate, 0.5 mL.min$^{-1}$; detection, (a) UV Detector (Agilent 1200, Agilent Technologies, Waldbronn, Germany) operating at wavelength of 280 nm, (b) multi-angle laser light scattering detector (Dawn multiangle Heleos TM, Wyatt Technology Corporation, Toulouse, France), and quasi elastic light scattering detector (QELS, Wyatt Technology), (c) interferometric refractometer (Optilab rEX, Wyatt Technology Corporation, Toulouse, France). 5 mg of each extracted fraction was dissolved in 1 mL of 0.1 M NaOH (titrated with HCl to pH 12) and filtered through a regenerated cellulose filter (porosity: 0.45 μm) before being injected into the HPSEC system.

#### 2.4.8. Gas chromatography-mass spectroscopy (GC–MS)

GC–MS analysis of the extracted fractions was performed using a TRACE 1310 gas chromatograph equipped with a ZB-5HT Inferno ™ capillary column (30 m × 0.25 mm inner diameter and 0.25 μm film thickness) and a single quadrupole Mass Spectrometer ISQ 7000. Helium was used as the carrier gas (flow rate: 2 mL·min$^{-1}$). The temperature of the injector was set at 320 °C. The temperature of the oven was kept at 70 °C for 5 min, and then increased at a rate of 5 °C·min$^{-1}$ to 320 °C and maintained at this temperature for 5 min. For the preparation of the sample for GC–MS, 10 mg of the extracted fractions was dissolved in 1 mL of 60 % ethanol overnight. The samples were then filtered using a 0.45 μm polytetrafluoroethylene (PTFE) filter. 500 μl ethyl acetate and 400 μl ultra-pure water were added to the aliquot and allowing time for two phases to appear. 100 μl was taken from the upper phase twice, placed in glass vials and dried under nitrogen. Silylation of the samples was done by adding 70 μl pyridine (Merck, Germany) and 30 μl *N*,*O*-Bis (trimethylsilyl) trifluoroacetamide (BSTFA) (Merck, Germany) to each sample and incubating at 60 °C for 30 min.

#### 2.4.9. Thermogravimetric analysis (TGA)

A thermogravimetric analysis of the extracted fractions was performed using Setaram Setsys 16/18 (SETARAM Instrumentation, France). 10 mg of sample was heated under a nitrogen atmosphere with a heating rate of 10 °C·min$^{-1}$ and a temperature ramp of 30 – 900 °C. The rate of weight loss is expressed as a function of temperature via derivative TG (DTG) curves.

#### 2.4.10. Statistical analysis

The statistical analysis of the results was performed by analysis of variance (ANOVA) using Statgraphics Centurion XVII-X64. Significance was established at a confidence level exceeding 95 % ($p < 0.05$).

## 3. Results and discussion

The initial raw material composition of the two tested biomass samples is shown in Table 1. Despite the diverse taxonomical origin of both biomasses, they had comparable amounts of lignin (20 – 25 %) as the main constituent after holocellulose. The relatively high lignin content and the availability of this biomass at very low cost points out their potential for lignin valorisation. Minor amounts of ashes, protein, and extractives were also found in both samples, with vine shoots having significantly higher amounts.

The ozone reaction with the biomass, during the process in the pilot-scale reactor, was monitored by measuring the pH, water activity ($a_w$), and temperature of the biomass at different ozonation times. Significant changes in pH and temperature confirmed the reaction of ozone with biomass.

### 3.1. Impact of ozone on pH during the ozonation process

Fig. 2a and 2b display pH variations observed during the ozonation of *Miscanthus giganteus* and vine shoots. These graphs provide a comprehensive overview of the relationship between ozonation time and pH, encompassing all experiments, including the control (blank) with oxygen. The graphs reveal that with 160 min of ozonation, *Miscanthus giganteus* pH dropped from 6.3 to 2.0 and stabilised, while vine shoots required 320 min to decrease the pH from 6.52 to a constant 2.10. These pH shifts are attributed to the ozone reaction with biomass, confirmed by the oxygen control's lack of pH impact. The observed pH reduction is the result of ozone reacting with the double bonds present in the biomass, since it readily reacts with compounds containing conjugated double bonds and high electron density functional groups. Lignin, rich in conjugated aromatic bonds, is highly susceptible to oxidation during ozonation, leading to the release of lower molecular weight soluble compounds, mainly organic acids such as formic and acetic acid, causing the drop in pH (García-Cubero et al., 2009). The lower rate of pH decline in vine shoots can be attributed to their larger particle size and/or different lignin structure. *Miscanthus giganteus* has a composition of 52 % G-units, 44 % S-units, and 4 % H-units, whereas vine shoots comprise 71 % G-units, 26 % S-units, and 3 % H-units (El Hage et al., 2009; Prozil et al., 2014). Ozone reacts more rapidly with syringyl groups compared to guaiacyl groups, potentially explaining the higher pH reduction rate in *Miscanthus giganteus* with more syringyl groups (Quesada et al., 2002).

**Table 1**
Chemical composition of *Miscanthus* and vine shoots biomasses used for ozonation.

| Chemical composition (%) | *Miscanthus* | Vine Shoots |
|---|---|---|
| Lignin | 22.35 (±0.03)$^{a,*}$ | 23.70 (±3.81)$^{a}$ |
| Holocellulose | 80.37 (±0.25)$^{a}$ | 72.00 (±4.4)$^{b}$ |
| Ash | 1.94 (±0.18)$^{b}$ | 4.28 (±0.19)$^{a}$ |
| Extractives | 3.11 (±0.23)$^{b}$ | 5.41 (±0.04)$^{a}$ |
| Protein | 1.40 (±0.25)$^{b}$ | 4.73 (±0.12)$^{a}$ |

(*) Values represent the average of independent replicates. Standard deviations are provided in parentheses. Different superscript letters (a-b) within the same raw indicate significant differences among formulations ($p < 0.05$).

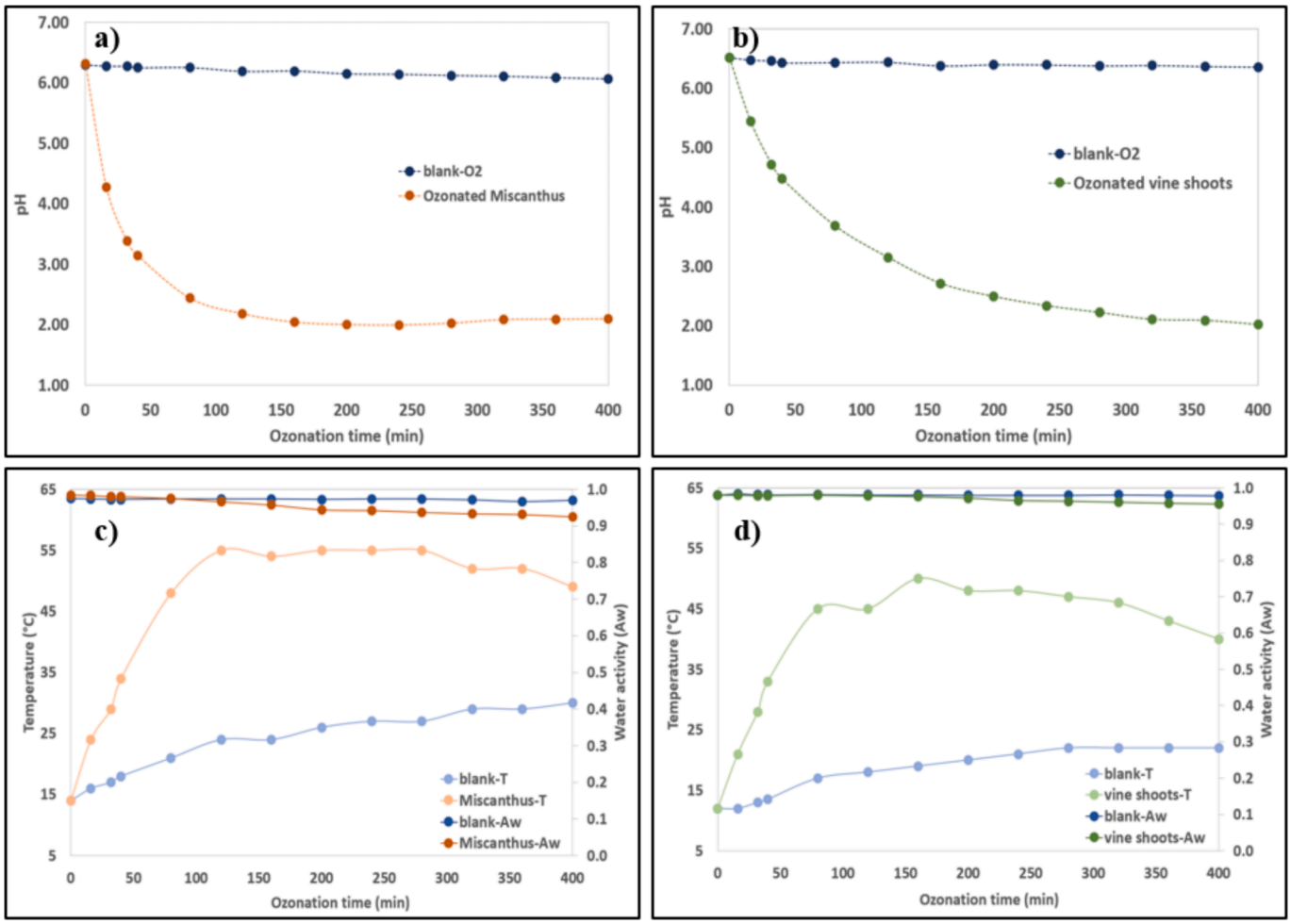


**Fig. 2.** A). ph time course during *Miscanthus* ozonation; b) pH time course during vine shoots ozonation; c) Time course of $a_w$ and temperature during ozonation of *Miscanthus*; d) Time course of $a_w$ and temperature during ozonation of vine shoots.

### 3.2. Water activity and temperature change during the ozonation process

Water activity ($a_w$) was monitored during ozonation to assess the ratio of free to bound water in the sample. Ozone, in its reaction with biomass, first diffuses into the free water present in the sample before transitioning to bound water, initiating the reaction. This highlights the significance of free water in facilitating ozone transfer to the biomass surface, a crucial factor in assessing the effectiveness of the ozone reaction with biomass (Choi et al., 2002). The initial water activity ($a_w$) of both *Miscanthus giganteus* and vine shoots was 0.98. This specific value was obtained after adding water to get homogenous samples within the reactor, which would facilitate the reaction of biomass with ozone. After 400 min of ozonation, both *Miscanthus giganteus* and vine shoots saw a slight decrease in water activity, from the initial 0.98 to 0.93 and 0.96, respectively (Fig. 2c and 2d). This decline in water activity is linked to the exothermic reaction between ozone and biomass resulting in an increase in temperature. The slight drop in $a_w$ suggests that ozone mass transfer remained consistent, indicating efficient ozone delivery to the sample surfaces and an effective reaction with the biomass.

Temperature monitoring of both biomasses during ozonation and oxygen blank experiments revealed some differences. The blank experiment showed a slight biomass temperature increase due to mechanical movement. Whereas, during ozonation, both *Miscanthus giganteus* and vine shoots initially exhibited a temperature rise, reaching a peak at 160 min (Fig. 2c and 2d). This rise was attributed to the exothermic ozone-biomass reaction, which subsequently stabilised after 320 min before gradually decreasing, possibly indicating that the reaction had reached its maximum potential.

### 3.3. Ozone consumption during the biomass ozonation process

The efficiency of the ozonation process is greatly influenced by the amount of ozone consumed per gram of dry biomass, which is regarded as the most crucial factor from an economic standpoint (Coca et al., 2016). The ozone consumption by *Miscanthus giganteus* and vine shoots during the ozonation process was calculated based on the recorded ozone inlet and outlet concentrations (Fig. A.1) as described by Eq. (1). Fig. 3a illustrates a linear relationship between the ozone consumption by the biomass and the ozonation time. As the ozonation time is extended both *Miscanthus giganteus* and vine shoots exhibit an increase in ozone consumption, with vine shoots consuming slightly less ozone than *Miscanthus giganteus* (Fig. 3a). Towards the end of the ozonation process, the total ozone consumption was determined to be 0.2489 g $O_3 \cdot g^{-1}$ of dry biomass for *Miscanthus giganteus*, whereas for vine shoots it was 0.2072 g $O_3 \cdot g^{-1}$ of dry biomass. The difference in ozone consumption between both biomasses could be attributed to the larger particle size of vine shoots, which reduced the specific area available for ozone reaction, along with the recalcitrant nature of this woody biomass.

### 3.4. Yield of extracted biomass fractions during the ozonation process

The efficiency of extraction from both biomasses using ozone was evaluated by assessing the extract yield (Eq. (2)). The extract yield

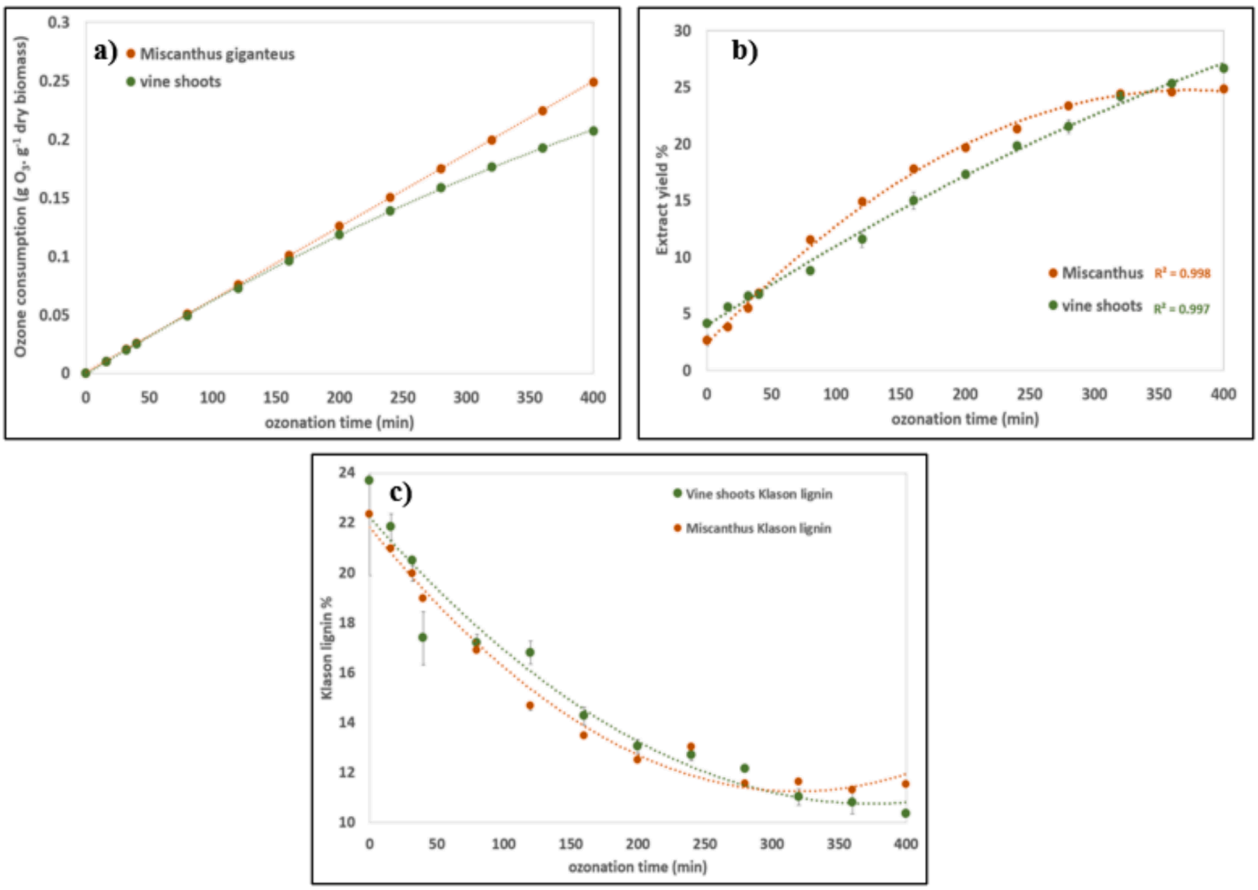


**Fig. 3.** a). ozone consumption by miscanthus and vine shoots during the ozonation process; b) the yield of extracted fractions obtained from miscanthus and vine shoots during the ozonation process; c) time course of klason lignin during the ozonation process of miscanthus and vine shoots.

represents the amount of biomass that reacted with ozone, underwent cleavage, and became extractable through water washing. Fig. 3b illustrates the evolution of the extract yield over the course of the ozonation process for both *Miscanthus giganteus* and vine shoots. As depicted in the graph, the yield of *Miscanthus giganteus* extract increased with increasing ozonation time, reaching a maximum of 24.4 % at 320 min. Thereafter, it remained stable for the rest of ozonation process, indicating the attainment of the highest possible extraction of *Miscanthus giganteus* under these conditions. On the other hand, for vine shoots, the extract yield continued to increase during ozonation to reach 26.7 % at the end of the ozonation process. The difference in extract yield between *Miscanthus giganteus* and vine shoots may be attributed to the structural differences between the two types of biomasses and their respective capacity for reaction with ozone.

### 3.5. Colour change of extracted biomass fractions during the ozonation process

During the ozonation process, noticeable changes in colour were observed in the extracted fractions, transitioning from brown to yellow, and eventually to a pale-yellow shade for the longest ozonised samples (Fig. A.2). The brown colour of the initial fractions comes from water-soluble lignin-derived phenolic compounds (Rosen et al., 2019). The reaction of ozone with *Miscanthus giganteus* and vine shoots leads to the release of oxidised compounds, mostly derived from lignin, and to a lesser extent from polysaccharides. The yellow colour observed in the extracted fractions can be attributed to the presence of carbonyl (CO) and carboxyl (COOH) groups within the oxidised compounds (Ahn et al., 2019).

### 3.6. Lignin extraction during the ozonation process

The lignin content in *Miscanthus giganteus* and vine shoots at different ozonation times is illustrated in Fig. 3c. Initially, the lignin content in *Miscanthus giganteus* experienced a sharp decrease from 22.35 % to 12.51 % within the first 200 min of ozonation, indicating a substantial reduction (44 %) with an ozone consumption of 0.1256 g $O_3 \cdot g^{-1}$ biomass. As the ozonation process continued, the reaction rate gradually decreased, revealing the existence of two distinct reaction phases. This two-phase behaviour of lignin extraction from biomass by the ozonation process has already been observed for other biomasses such as wheat bran or cereal straw in lab-scale fixed-bed reactors. In the case of wheat bran, a 40 % reduction in Klason lignin was observed after 120 min ozonation with an ozone consumption of 0.209 g $O_3 \cdot g^{-1}$ dry biomass (Li et al., 2021). García-Cubero et al (2012) reported a similar lignin extraction behaviour from cereal straw with a Klason lignin decreasing from 23 % to 10.8 % after 150 min of reaction (García-Cubero et al., 2012).

In the first phase of reaction, up to 200 min (Fig. 3c), the lignin extraction was highly related to ozone consumption. This suggests that ozone reacted preferentially with easily accessible unsaturated bonds from lignin, effectively extracting lignin fractions from *Miscanthus giganteus*. During the second phase (Fig. 3c), the reaction rate of ozone with lignin decreased, likely due to the involvement of less reactive bonds. Although the lignin extraction decreased in the second phase, the ozone consumption continued to rise. This could be attributed to ozone reacting with the previously extracted lignin fractions, breaking them down into lower molecular weight compounds (García-Cubero et al., 2012). Additionally, the ozone may have reacted with other compounds available in the biomass, such as hemicelluloses, resulting in their

extraction from *Miscanthus giganteus* (Travaini et al., 2013). A similar behaviour was observed in the vine shoots, with a different lignin structure than *Miscanthus giganteus* (Fig. 3c). Both phases of lignin extraction were also evident. The first 280 min of ozonation exhibited a high extraction rate, reducing lignin from 23.70 % to 12.17 %, followed by a gradual drop-in rate until the ozonation process was complete. Comparing the lignin extraction from both *Miscanthus giganteus* and vine shoots, it is evident that ozone elicited similar behaviour with comparable extraction rates. This consistency could be attributed to the high oxidation potential of ozone.

The extracted lignin from biomass was presented as lignin degradation products, which could include lignin oligomers and phenolic monomers in the extracted fractions. The purity of the degraded lignin in the extracted fractions for both biomasses is summarized in Table A1. It is evident from the table that the purity of lignin in the extracts increased until certain point in time, after which it experienced a reduction until the end of ozonation. This reduction could be attributed to the extraction of hemicelluloses with extended ozonation time. Notably, vine shoots extracts exhibited a higher purity of lignin compared to *Miscanthus*, possibly due to structural differences between grass-type and woody biomasses.

### 3.7. ATR-FTIR analysis of structural changes of extracted fractions during the ozonation process

FTIR spectroscopy has been used to better understand the reaction of ozone with lignin-extracted fractions during the ozonation process. Fig. 4 shows the progression of the structural changes in these fractions over time, while the corresponding spectral data and their signal allocations are presented in Table 2. The analysis of Fig. 4 shows notable changes in various bands ranging from 1900 to 800 $cm^{-1}$. Initially, the composition of the extracts from *Miscanthus giganteus* and vine shoots differed at time zero due to the distinct structures of the biomasses – one grassy and the other woody (*Miscanthus giganteus* and vine shoots, respectively). In the case of *Miscanthus giganteus* extracts, the aromatic structure initially appeared at 1600 and 1510 $cm^{-1}$, whereas for vine shoots extracts, it only appeared at 1600 $cm^{-1}$. The 1510 $cm^{-1}$ band represents the electron donor structure of aromatic compounds (Socrates, 2010), showing that *Miscanthus giganteus* releases more electron donor aromatics that can further react with ozone. As the ozonation time increased from 0 to 400 min, and the intensity of the aromatic peaks (1510 and 1600 $cm^{-1}$) decreased regardless of the biomass type. Simultaneously, there was an increase in the peak at 1730 $cm^{-1}$ due to the carbonyl stretching of the unconjugated ketone and carboxyl groups (Fig. 4) (Bule et al., 2013; Liao et al., 2021). The reduction in aromatic peaks was attributed to the interaction between ozone and the extracted lignin fractions, causing oxidation and prompting a ring-opening reaction via the Criegee mechanism (Travaini et al., 2016b). Furthermore, the vine shoot extracts displayed a shift from 1600 to 1640 $cm^{-1}$ with prolonged ozonation. This change results from the generation of conjugated carbonyl groups in the woody biomass extracts (Bule et al., 2013). However, such a shift was not observed in the *Miscanthus giganteus* extracts. Another interesting change was the increase in the peak at 1236 $cm^{-1}$ for both extracts. This peak is related to syringyl groups, indicating the extraction of this lignin unit in both biomasses (Barrera-Martínez et al., 2016). The changes observed in the FTIR spectra of extracted lignin fractions showed that ozone reacted simultaneously with lignin in both biomasses (according to the results on Klason lignin) (Fig. 3c) and extracted lignin fractions of the biomass as early, as the start of the process.

**Table 2**
Peak assignment in the ATR-FTIR spectra of *Miscanthus* and vine shoot extracts resulting from the ozonation process.

| Vibration type and functional groups | Wavenumber ($cm^{-1}$) | References |
|---|---|---|
| C = O stretching (unconjugated ketone, ester or carboxylic groups) | 1725–1730 | (Hoareau et al., 2004), (Socrates, 2010) |
| C = O stretching (conjugated carbonyl groups) | 1640 | (Hortling et al., 1997; Shi et al., 2012) |
| Aromatic skeletal vibrations, (lignin) | 1600 | (Xu et al., 2013), (Perrone et al., 2016), (Socrates, 2010) |
| Aromatic skeletal vibrations, (lignin) | 1510 | (Xu et al., 2013), (Perrone et al., 2016), (Socrates, 2010) |
| Aromatic ring and C = C stretching | 1454 | (Barrera-Martínez et al., 2016), (Perrone et al., 2016) |
| Syringyl phenol C-OH in lignin and xylan | 1236 | (Socrates, 2010), (Barrera-Martínez et al., 2016) |

### 3.8. SEC molecular weight analysis of fractions extracted from lignin during the ozonation process

Fig. A.3 (supplementary material) shows the SEC results of the cumulative molecular weight fractions of lignin oligomers extracted from *Miscanthus giganteus* and vine shoots at different ozonation times. The results suggest that ozone reacted with the lignin extracted from both biomasses causing its gradual decomposition into lower molecular weight fractions, as shown earlier by FTIR analysis (Fig. 4). This reaction occurs in parallel with that of ozone reacting with the lignin present in the starting biomass, which was confirmed by the results on Klason lignin. Thus, the ozone reacts with both the original lignin present in the biomass and on the lignin extracted from the biomass during the ozonation process.

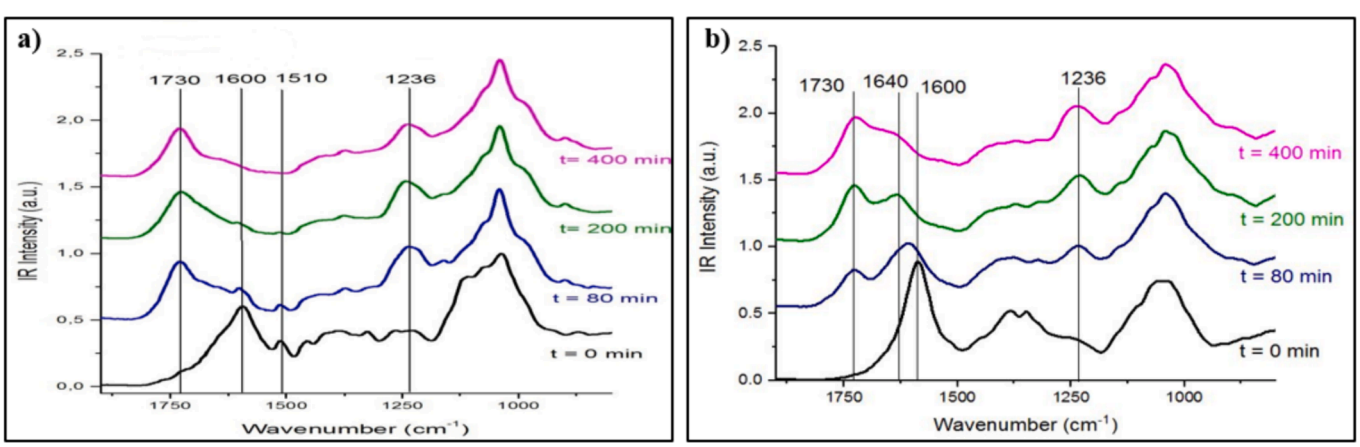


**Fig. 4.** ATR-FTIR spectra of a) *Miscanthus* and b) vine shoots extracted fraction obtained at different ozonation times.

The molecular weight ($M_w$) of lignin oligomers from both biomasses rapidly decreased during the first 160 min of ozonation, after which it stabilised until the end of the process (Fig. A.4 a). The slower rate of molecular weight reduction after 160 min of ozonation can be attributed to the presence of inter-aromatic C–C bonds in the lignin oligomers, which resist the ozone reaction. For *Miscanthus giganteus*, the Mw of lignin oligomers decreased from 11,000 to 2,600 g·mol$^{-1}$ (76.4 % reduction) in the first 160 min of ozonation, while for vine shoots it decreased from 17,000 to 5,300 g·mol$^{-1}$ (68.8 % reduction) (Table 3). The higher molecular weight of lignin oligomers in vine shoots compared to *Miscanthus giganteus* is due to the distinct initial structure of lignin in these biomass types, with *Miscanthus giganteus* being a grass, and vine shoots being a woody biomass. This observation confirms the differences seen in the FTIR analysis that were noticed in the extracted fractions, which depict the production of conjugated carbonyl groups in grapevine shoot extracts (Fig. 4). Similar results were observed after the ozonation of technical lignins obtained by other delignification processes such as Kraft, organosolv, pyrolysis, and alkaline processes. Figueirêdo et al. (2019) studied the ozonation of pyrolytic lignin and observed a 40 % decrease in lignin molecular weight after 4 h of ozonation. They also studied the ozone reaction with four different technical lignins (Indulin-AT Kraft, ball-milled Indulin-AT Kraft, Alcell organosolv, and Fabiola organosolv), observing a 40 – 70 % decrease in the molecular weight of the studied lignins when extending the ozonation time (Figueirêdo et al., 2020a). Du et al. (2022) also observed a decrease in the molecular weight of Kraft lignin from 1875 to 1616 g·mol$^{-1}$ after 40 min ozonation with a flow rate of 7 g·h$^{-1}$. Wang et al. (2022) reported a decrease in the weight average molecular weight of alkali lignin from 14,116 g·mol$^{-1}$ to 10,667 g·mol$^{-1}$ after 45 min of ozonation at pH 3.

To investigate the homogeneity of the extracted lignin oligomers obtained at different ozonation times, the polydispersity index was considered (Table 3). According to the results, at the beginning of the ozonation process more heterogeneous lignin oligomers were extracted. However, after an extended ozonation time, the ozone reacts with the lignin extracted fractions, breaking them down into lower molecular weight compounds, resulting in more homogeneous extracts. Nevertheless, the lignin oligomeric fractions from vine shoots presented a higher polydispersity than those of *Miscanthus giganteus*, indicating a greater heterogeneity of their fractions.

As for the mass fraction of lignin oligomers, it is determined by dividing the calculated mass of lignin oligomers using SEC by the injected mass to the column. Mass fraction of lignin oligomers increased during the ozonation process (Table 3), suggesting the release of more lignin oligomers as ozonation progressed. According to this table, a higher mass fraction of lignin oligomers was obtained from vine shoots compared to *Miscanthus giganteus*. At the end of the ozonation process, 44.4 % of lignin oligomers were extracted from vine shoots, while 33.5 % were obtained from *Miscanthus giganteus*.

### 3.9. Ozone reaction products from Miscanthus giganteus and vine shoots characterised by GC–MS

Analysis of the phenolic monomers and organic acids resulting from reaction with ozone was carried out by GC–MS. Several types of organic acids, phenolic acids, and phenolic aldehydes were identified at various times during ozonation (Fig. 5). Table 4 provides insights into the structures, molecular weights, and oxidation mechanisms of the ozone oxidation products (Musl et al., 2019; Quesada et al., 1998).

The divergence of phenolic monomers produced during the ozonation process of *Miscanthus giganteus* and vine shoots is attributed to their distinct initial lignin structures. Specifically, extracts from *Miscanthus giganteus* released two phenolic monomers: 4-hydroxybenzaldehyde and 4-hydroxybenzoic acid. These arise from the reaction of ozone with the olefinic bond between the α and β carbons in the p-coumaric acid of acylated lignin, leading to the formation of 4-hydroxybenzaldehyde and/or 4-hydroxybenzoic acid during cleavage (Danby et al., 2018). A lower amount of hydroquinone and vanillin were also released due to the side chain cleavage (Quesada et al., 1998). On the other hand, vine shoots exhibited a lower release of phenolic monomers during ozonation compared to *Miscanthus giganteus*. This difference arises from the lignins derived from woody biomass, which are partially acetylated at the gamma position of the alkyl side chain. Consequently, the presence of peripheral aromatic groups linked to olefins, capable of generating aromatic monomers during ozone treatment, is limited (Danby et al., 2018). In the initial composition of the vine shoot extract, the primary phenolic compounds identified were resveratrol and catechin.

The ozone oxidation process yielded a range of organic acids including oxalic acid, glycolic, glyceric, acetic, tartaric, malic, and lactic acids. Previous research has indicated that aldehyde and ketone-type compounds can undergo further oxidative degradation, resulting in acid-type compounds (Eriksson and Gierer, 1985). As observed, with increased ozonation time, the pH of the extract decreased significantly. The drop in pH was primarily attributed to carboxylic acids resulting from significant lignin degradation (Liao et al., 2021). Oxalic acid was formed by extensive oxidation of the aromatic structure; however, its concentration can decrease with longer ozonation time, possibly due to excessive oxidation leading to $CO_2$ formation (Figueirêdo et al., 2020b). In this study, the generation of oxalic acid was increased by extending the ozonation of vine shoots until the end of process. In contrast, for *Miscanthus giganteus*, oxalic acid decreased after 240 min of ozonation.

The oxidation of lignin has given rise to a range of products, including aromatic acids, aldehydes, phenolic building blocks, and dicarboxylic acids (DCAs). These compounds have potential

**Table 3**
Weight-average (Mw) and number-average (Mn) molecular weight, polydispersity and mass fraction of lignin oligomers obtained at different ozonation times from *Miscanthus giganteus* and vine shoots.

| Ozonation time (min) | *Miscanthus giganteus* $M_w$ (g.mol$^{-1}$) | $M_n$ (g.mol$^{-1}$) | $M_w/M_n$ | Mass fraction (%) | Vine shoots $M_w$ (g.mol$^{-1}$) | $M_n$ (g.mol$^{-1}$) | $M_w/M_n$ | Mass fraction (%) |
|---|---|---|---|---|---|---|---|---|
| 0 | 11,000 | 4000 | 2.700 | 17.8 | 17,000 | 3200 | 5.342 | 23.1 |
| 16 | 11,000 | 5600 | 1.938 | 28.0 | 15,000 | 4000 | 3.826 | 28.2 |
| 32 | 7600 | 4000 | 1.884 | 30.8 | 14,000 | 4400 | 3.232 | 33.6 |
| 40 | 6400 | 3300 | 1.921 | 33.8 | 11,000 | 3700 | 2.962 | 35.6 |
| 80 | 3700 | 1900 | 1.956 | 35.3 | 8800 | 3500 | 2.506 | 39.9 |
| 120 | 3500 | 1700 | 2.037 | 36.1 | 6400 | 2500 | 2.544 | 43.9 |
| 160 | 2600 | 1200 | 2.201 | 36.3 | 5300 | 2100 | 2.509 | 45.0 |
| 200 | 2200 | 1100 | 2.118 | 38.1 | 4700 | 1800 | 2.694 | 46.0 |
| 240 | 2100 | 1000 | 2.005 | 38.9 | 4300 | 1600 | 2.673 | 43.7 |
| 280 | 1900 | 1000 | 1.847 | 38.9 | 4000 | 1500 | 2.724 | 44.6 |
| 320 | 1700 | 900 | 1.830 | 37.8 | 3600 | 1300 | 2.697 | 44.6 |
| 360 | 1500 | 800 | 1.815 | 34.4 | 3600 | 1300 | 2.868 | 43.0 |
| 400 | 1500 | 800 | 1.804 | 33.5 | 3600 | 1300 | 2.742 | 44.4 |

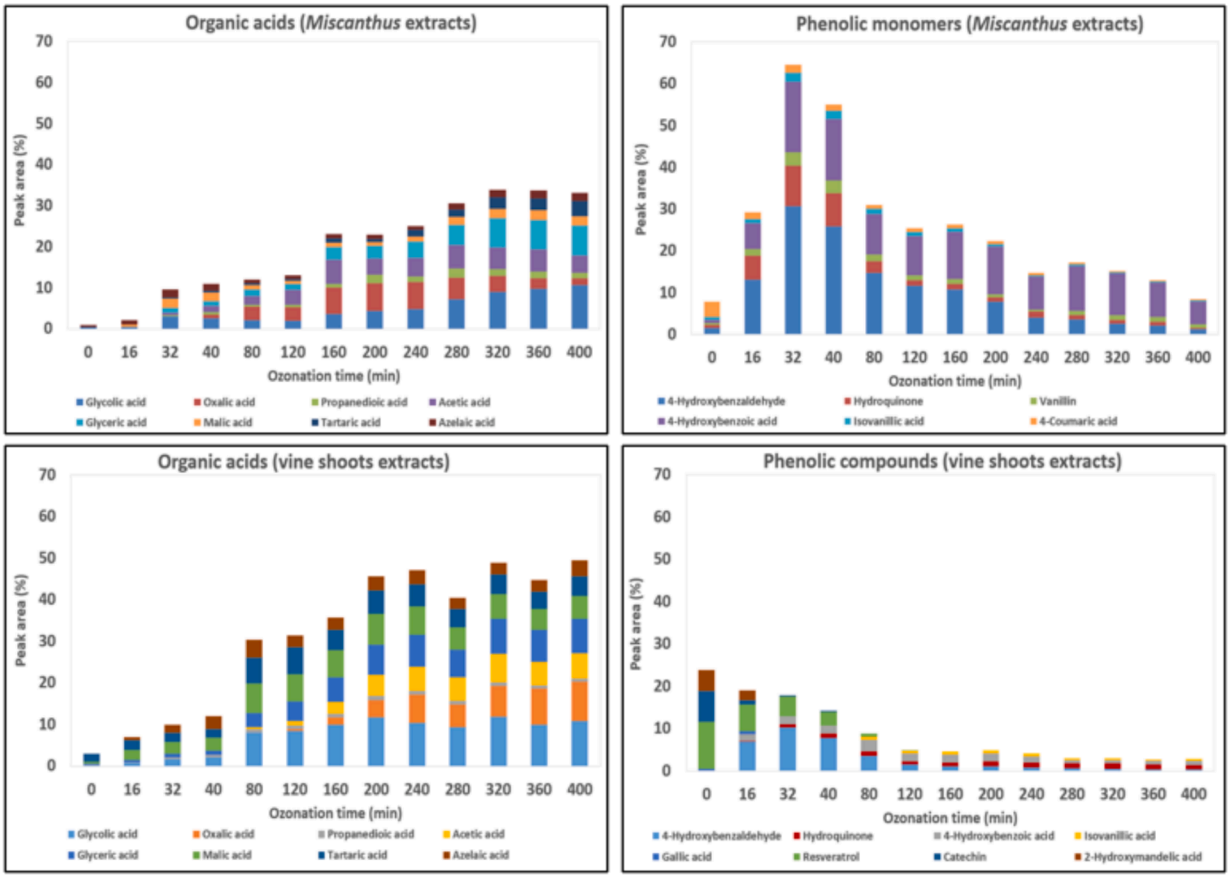


**Fig. 5.** The relative content of phenolic monomers and organic acids obtained during the ozonation of *Miscanthus* and vine shoots and quantified by GC–MS.

applications in diverse fields, such as chemicals, fuels, and additives (Figueirêdo et al., 2020a).

### *3.10. Thermogravimetric analysis (TGA) of extracted fractions from ozonation of Miscanthus giganteus and vine shoots*

Thermogravimetric analysis was used for assessing the thermal stability of the extracted fractions (Du et al., 2022). Fig. 6 shows the thermogravimetric curves of the extracted fractions derived from *Miscanthus giganteus* and vine shoots at different ozonation times. TGA results of these extracts revealed a mixture of various components described below. Notably, the *Miscanthus giganteus* extracts presented a more uniform structure compared to vine shoot extracts. The homogeneity of the thermogram for vine shoot extracts improved with longer ozonation times, which is consistent with the results of the SEC analysis.

Before ozonation, *Miscanthus giganteus* extracts showed a peak between 50 to 200 °C and another between 200 to 350 °C, likely corresponding to water-soluble compounds, such as tannins, or hemicellulose fractions, respectively, which partially dissolve in water after mechanical grinding. On the other hand, vine shoots showed two peaks between 50 and 200 °C and one peak between 200 and 350 °C. With prolonged ozonation time, a signal of thermal degradation in the range of 70 to 230 °C increases, which is in consistent with the increase presence of the lower molecular weight compounds (Table 3) possibly lignin oligomers.

The original lignin present in the biomass generally decomposes at temperatures ranging from 392 to 540 °C (Rosen et al., 2019). The TGA results (Fig. 6) indicate that the extracted fractions have a lower molecular weight and are more volatile than the original lignin present in the biomass. The maximum mass loss temperature was around 200 °C, corresponding to the decomposition temperature of lower molecular weight compounds. Moreover, FTIR analysis revealed the presence of carbonyl and carboxyl groups in the extracted lignin fractions after ozonation. According to Du et al. (2022), the decarboxylation and decarbonylation reactions occur in the temperature range of 150 – 250 °C, leading to the formation of a peak in this temperature range. Therefore, regardless of the type of biomass, the ozonation process makes it possible to extract thermally stable and homogeneous fractions. These extracts, stable at 200 °C, are promising for future applications.

According to the literature, the ozonation of technical lignins produced extracted lignin fractions with different thermal stability. Figueirêdo et al., (2020b) obtained low molecular weight lignin fractions with the maximum rate of weight loss around 100 °C by ozonation of Klason, ball-milled, and organosolv lignin. The plasma-based ozonation of alkaline lignin by Muazzam et al. (2023) generated low molecular weight compounds with the maximum rate of weight loss around 250 °C, due to the carbonisation of the aromatic structure.

## 4. Conclusions

This study highlights the use of ozonation in a 200 L twin-shaft paddle mixer reactor to efficiently extract lignin from both wood and grass lignocellulosic biomass sources. The reactor's uniform mixing capability ensures consistent ozone interaction, producing an extraction of approximately 48 % lignin from both types of biomass without the use of chemical solvents. The ozonation generates lignin oligomers, phenolic monomers, and organic acids, with vine shoots producing higher molecular weight lignin oligomers. Importantly, the resulting lignin oligomers exhibit excellent thermal stability up to 200 °C, promising potential applications. Ozonation proves to be an environmentally-friendly method for sustainable lignin extraction.

**Table 4**
Ozone reaction products and the mechanism of oxidative degradation of lignin derived compounds.

| Compound | | Retention time (min) | Molecular weight (g.mol$^{-1}$) | Structure | Ozone reaction mechanism |
|---|---|---|---|---|---|
| Phenolic compounds | 4-Hydroxybenzaldehyde | 12.4 | 122.12 | 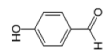 | Side chain cleavage (Musl et al., 2019; Quesada et al., 1998) |
| | Hydroquinone | 13.2 | 110.11 | 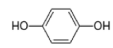 | |
| | Vanillin | 16.2 | 152.15 | 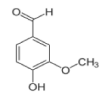 | |
| | 4-Hydroxybenzoic acid | 18.4 | 138.12 | 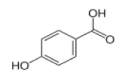 | |
| | Isovanillic acid | 21.4 | 168.15 | 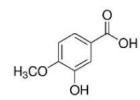 | |
| | 4-Coumaric acid | 24.9 | 164.16 | 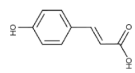 | |
| | Gallic acid | 25.6 | 170.12 | 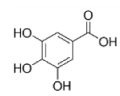 | |
| | Resveratrol | 37.9 | 228.25 | 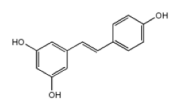 | |
| | Catechin | 40.6 | 290.26 | 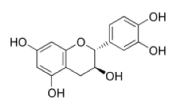 | |
| Organic acids | Glycolic acid | 5.8 | 76.05 | 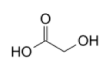 | Side chain cleavage (Musl et al., 2019; Quesada et al., 1998) |
| | Glyceric acid | 11.7 | 106.08 | 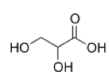 | |
| | Oxalic acid | 7.0 | 90.03 | 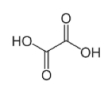 | Ring opening (Quesada et al., 1998) |
| | Propanedioic acid | 8.6 | 104.06 | 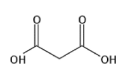 | |
| | Acetic acid | 9.8 | 60.05 | | |
| | Malic acid | 15.6 | 134.09 | 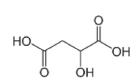 | Hydroquinone oxidation (Musl et al., 2019; Quesada et al., 1998) |
| | Tartaric acid | 19.2 | 150.09 | 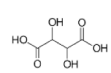 | |

## CRediT authorship contribution statement

**M. Ebrahimi:** Writing – original draft, Investigation, Formal analysis, Data curation. **V. Acha:** Writing – review & editing, Validation, Supervision, Conceptualization. **L. Hoang:** Resources, Methodology. **A. Martínez-Abad:** Writing – review & editing, Validation, Conceptualization. **A. López-Rubio:** Writing – review & editing, Validation, Conceptualization. **L. Rhazi:** Resources, Methodology. **T. Aussenac:** Writing – review & editing, Supervision, Project administration, Funding acquisition, Conceptualization.

## Declaration of competing interest

The authors declare the following financial interests/personal

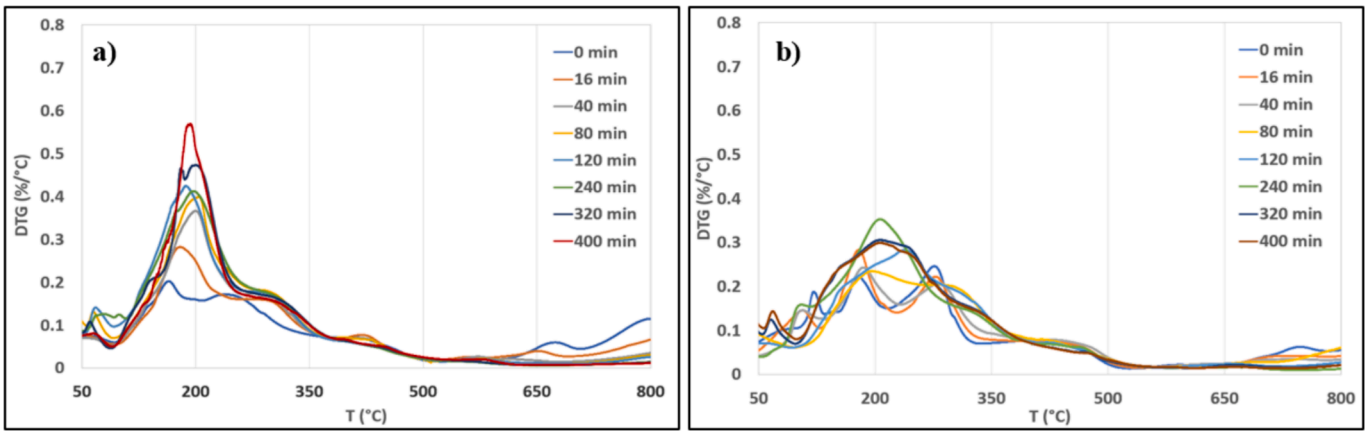


**Fig. 6.** TGA results of the extracted fractions obtained after ozonation from *Miscanthus* (a), and vine shoots (b).

relationships which may be considered as potential competing interests: AUSSENAC Thierry reports financial support was provided by Hauts-de-France Regional Council. If there are other authors, they declare that they have no known competing financial interests or personal relationships that could have appeared to influence the work reported in this paper.

## Data availability

Data will be made available on request.

## Acknowledgements

The authors are grateful for the financial support of Hauts-de-France region and UniLaSalle, France, and also the SO and Vine Box projects, Spain. Benoit Lerzy and Annaëlle Buchou are acknowledged for their valuable contributions in technical assistance.

## Appendix A. Supplementary data

Supplementary data associated with this article can be found, in the online version, at https://doi.org/10.1016/j.biortech.2024.130804.

## References

Ahn, K., Zaccaron, S., Zwirchmayr, N.S., Hettegger, H., Hofinger, A., Bacher, M., Henniges, U., Hosoya, T., Potthast, A., Rosenau, T., 2019. Yellowing and brightness reversion of celluloses: CO or COOH, who is the culprit? Cellulose. 26, 429–444.

Alzagameem, A., Bergrath, J., Rumpf, J., Schulze, M., 2022. Lignin-based composites for packaging applications, in: Micro and Nanolignin in Aqueous Dispersions and Polymers. Elsevier, pp. 131–171.

Ariyanta, H.A., Santoso, E.B., Suryanegara, L., Arung, E.T., Kusuma, I.W., Azman Mohammad Taib, M.N., Hussin, M.H., Yanuar, Y., Batubara, I., Fatriasari, W., 2023. Recent Progress on the Development of lignin as future ingredient biobased cosmetics. Sustain. Chem. Pharm. 32, 100966.

Bajwa, D.S., Pourhashem, G., Ullah, A.H., Bajwa, S.G., 2019. A concise review of current lignin production, applications, products and their environmental impact. Ind. Crop. Prod. 139, 111526.

Barrera-Martínez, I., Guzmán, N., Peña, E., Vázquez, T., Cerón-Camacho, R., Folch, J., Honorato Salazar, J.A., Aburto, J., 2016. Ozonolysis of alkaline lignin and sugarcane bagasse: Structural changes and their effect on saccharification. Biomass Bioenerg. 94, 167–172.

Becker, J., Wittmann, C., 2019. A field of dreams: Lignin valorization into chemicals, materials, fuels, and health-care products. Biotechnol. Adv. 37, 107360.

Benito-González, I., Jaén-Cano, C.M., López-Rubio, A., Martínez-Abad, A., Martínez-Sanz, M., 2020. Valorisation of vine shoots for the development of cellulose-based biocomposite films with improved performance and bioactivity. Int. J. Biol. Macromol. 165, 1540–1551.

Bule, M.V., Gao, A.H., Hiscox, B., Chen, S., 2013. Structural Modification of Lignin and Characterization of Pretreated Wheat Straw by Ozonation. J. Agric. Food Chem. 61, 3916–3925.

Capolupo, L., Faraco, V., 2016. Green methods of lignocellulose pretreatment for biorefinery development. Appl. Microbiol. Biotechnol. 100, 9451–9467.

Choi, H., Lim, H.-N., Kim, J., Hwang, T.-M., Kang, J.-W., 2002. Transport characteristics of gas phase ozone in unsaturated porous media for in-situ chemical oxidation. J. Contam. Hydrol. 57, 81–98.

Coca, M., González-Benito, G., García-Cubero, M.T., 2016. Chemical Oxidation With Ozone as an Efficient Pretreatment of Lignocellulosic Materials, in: Biomass Fractionation Technologies for a Lignocellulosic Feedstock Based Biorefinery. Elsevier, pp. 409–429.

Danby, A.M., Lundin, M.D., Subramaniam, B., 2018. Valorization of Grass Lignins: Swift and Selective Recovery of Pendant Aromatic Groups with Ozone. ACS Sustainable Chem. Eng. 6, 71–76.

Dong, X., Dong, M., Lu, Y., Turley, A., Jin, T., Wu, C., 2011. Antimicrobial and antioxidant activities of lignin from residue of corn stover to ethanol production. Ind. Crop. Prod. 34, 1629–1634.

Du, X., Wu, S., Li, T., Yin, Y., Zhou, J., 2022. Ozone oxidation pretreatment of softwood kraft lignin: An effective and environmentally friendly approach to enhance fast pyrolysis product selectivity. Fuel Process. Technol. 231, 107232.

El Hage, R., Brosse, N., Chrusciel, L., Sanchez, C., Sannigrahi, P., Ragauskas, A., 2009. Characterization of milled wood lignin and ethanol organosolv lignin from miscanthus. Polym. Degrad. Stab. 94, 1632–1638.

Eriksson, T., Gierer, J., 1985. Studies on the Ozonation of Structural Elements in Residual Kraft Lign Ins. J. Wood Chem. Technol. 5, 53–84.

Figueirêdo, M.B., Deuss, P.J., Venderbosch, R.H., Heeres, H.J., 2019. Valorization of Pyrolysis Liquids: Ozonation of the Pyrolytic Lignin Fraction and Model Components. ACS Sustainable Chem. Eng. 7, 4755–4765.

Figueirêdo, M.B., Heeres, H.J., Deuss, P.J., 2020. Ozone mediated depolymerization and solvolysis of technical lignins under ambient conditions in ethanol. Sustain. Energy Fuels. 4, 265–276.

Figueiredo, P., Lintinen, K., Kiriazis, A., Hynninen, V., Liu, Z., Bauleth-Ramos, T., Rahikkala, A., Correia, A., Kohout, T., Sarmento, B., Yli-Kauhaluoma, J., Hirvonen, J., Ikkala, O., Kostiainen, M.A., Santos, H.A., 2017. In vitro evaluation of biodegradable lignin-based nanoparticles for drug delivery and enhanced antiproliferation effect in cancer cells. Biomaterials. 121, 97–108.

García-Cubero, M.T., González-Benito, G., Indacoechea, I., Coca, M., Bolado, S., 2009. Effect of ozonolysis pretreatment on enzymatic digestibility of wheat and rye straw. Bioresoure Technol. 100, 1608–1613.

García-Cubero, M.T., Palacín, L.G., González-Benito, G., Bolado, S., Lucas, S., Coca, M., 2012. An analysis of lignin removal in a fixed bed reactor by reaction of cereal straws with ozone. Bioresource Technol. 107, 229–234.

Garlapati, V.K., Chandel, A.K., Kumar, S.P.J., Sharma, S., Sevda, S., Ingle, A.P., Pant, D., 2020. Circular economy aspects of lignin: Towards a lignocellulose biorefinery. Renew. Sust. Energ. Rev. 130, 109977.

Hoareau, W., Trindade, W.G., Siegmund, B., Castellan, A., Frollini, E., 2004. Sugar cane bagasse and curaua lignins oxidized by chlorine dioxide and reacted with furfuryl alcohol: characterization and stability. Polym. Degrad. Stabil. 86, 567–576.

Hortling, B., Tamminen, T., Kenttä, E., 1997. Determination of Carboxyl and Non-Conjugated Carbonyl Groups in Dissolved and Residual Lignins by IR Spectroscopy. Holzforschung 51, 405–410.

Li, C., Wang, L., Chen, Z., Li, Y., Luo, X., Zhao, F., 2021. Ozonolysis of wheat bran in subcritical water for enzymatic saccharification and polysaccharide recovery. The J. Supercritic. Fluids. 168, 105092.

Liao, J., He, S., Mo, L., Guo, S., Luan, P., Zhang, X., Li, J., 2021. Mass-production of high-yield and high-strength thermomechanical pulp fibers from plant residues enabled by ozone pretreatment. J. Clean. Prod. 296, 126575.

Maurya, D.P., Singla, A., Negi, S., 2015. An overview of key pretreatment processes for biological conversion of lignocellulosic biomass to bioethanol. 3 Biotech. 5, 597–609.

Muazzam, R., Hafeez, A., Uroos, M., Saeed, M., Rehman, F., Muhammad, N., 2023. Plasma-based ozonolysis of lignin waste materials for the production of value-added chemicals. Biomass Conv. Bioref. 13, 5903–5919.

Musl, O., Holzlechner, M., Winklehner, S., Gübitz, G., Potthast, A., Rosenau, T., Böhmdorfer, S., 2019. Changing the Molecular Structure of Kraft Lignins—Ozone Treatment at Alkaline Conditions. ACS Sustainable Chem. Eng. 7, 15163–15172.

Perrone, O.M., Colombari, F.M., Rossi, J.S., Moretti, M.M.S., Bordignon, S.E., Nunes, C.D. C.C., Gomes, E., Boscolo, M., Da-Silva, R., 2016. Ozonolysis combined with ultrasound as a pretreatment of sugarcane bagasse: Effect on the enzymatic saccharification and the physical and chemical characteristics of the substrate. Bioresource Technol. 218, 69–76.

Prozil, S.O., Evtuguin, D.V., Silva, A.M.S., Lopes, L.P.C., 2014. Structural Characterization of Lignin from Grape Stalks (Vitis vinifera L.). J. Agric. Food Chem. 62, 5420–5428.

Quesada, J., Rubio, M., Gómez, D., 1998. Ozonation Products of Organosolvolytic Extracts from Vegetal Materials. J. Agric. Food Chem. 46, 692–697.

Quesada, J., Teffo-Bertaud, F., Croué, J.P., Rubio, M., 2002. Ozone Oxidation and Structural Features of an Almond Shell Lignin Remaining after Furfural Manufacture. Holzforschung 56, 32–38.

Rajesh Banu, J., Kavitha, S., Yukesh Kannah, R., Poornima Devi, T., Gunasekaran, M., Kim, S.-H., Kumar, G., 2019. A review on biopolymer production via lignin valorization. Bioresource Technol. 290, 121790.

Rice, R.G., Netzer, A. (Eds.), 1982. Handbook of Ozone Technology and Applications. Ann Arbor Science, Ann Arbor, Mich.

Rosen, Y., Mamane, H., Gerchman, Y., 2019. Short Ozonation of Lignocellulosic Waste as Energetically Favorable Pretreatment. Bioenerg. Res. 12, 292–301.

Shi, F., Xiang, H., Li, Y., 2015. Combined pretreatment using ozonolysis and ball milling to improve enzymatic saccharification of corn straw. Bioresource Technol. 179, 444–451.

Shi, J., Xing, D., Lia, J., 2012. FTIR Studies of the Changes in Wood Chemistry from Wood Forming Tissue under Inclined Treatment. Energy Procedia. 16, 758–762.

Socrates, G., 2010. Infrared and Raman characteristic group frequencies: tables and charts, 3. ed., repr. as paperback. ed. Wiley, Chichester.

Travaini, R., Otero, M.D.M., Coca, M., Da-Silva, R., Bolado, S., 2013. Sugarcane bagasse ozonolysis pretreatment: Effect on enzymatic digestibility and inhibitory compound formation. Bioresource Technol. 133, 332–339.

Travaini, R., Barrado, E., Bolado-Rodríguez, S., 2016a. Effect of ozonolysis pretreatment parameters on the sugar release, ozone consumption and ethanol production from sugarcane bagasse. Bioresource Technol. 214, 150–158.

Travaini, R., Martín-Juárez, J., Lorenzo-Hernando, A., Bolado-Rodríguez, S., 2016b. Ozonolysis: An advantageous pretreatment for lignocellulosic biomass revisited. Bioresource Technol. 199, 2–12.

van der Cruijsen, K., Al Hassan, M., van Erven, G., Dolstra, O., Trindade, L.M., 2021. Breeding Targets to Improve Biomass Quality in Miscanthus. Molecules 26, 254.

Wang, T., Li, H., Diao, X., Lu, X., Ma, D., Ji, N., 2023. Lignin to dispersants, adsorbents, flocculants and adhesives: A critical review on industrial applications of lignin. Ind. Crop. Prod. 199, 116715.

Wang, H., Zhao, L., Ren, J., He, B., 2022. Structural Changes of Alkali Lignin under Ozone Treatment and Effect of Ozone-Oxidized Alkali Lignin on Cellulose Digestibility. Processes 10, 559.

Wu, J., Upreti, S., Ein-Mozaffari, F., 2013. Ozone pretreatment of wheat straw for enhanced biohydrogen production. Int. J. Hydrogen Energ. 38, 10270–10276.

Xu, F., Yu, J., Tesso, T., Dowell, F., Wang, D., 2013. Qualitative and quantitative analysis of lignocellulosic biomass using infrared techniques: A mini-review. Appl. Energ. 104, 801–809.

Zhang, M., Tian, R., Tang, S., Wu, K., Wang, B., Liu, Y., Zhu, Y., Lu, H., Liang, B., 2023. The structure and properties of lignin isolated from various lignocellulosic biomass by different treatment processes. Int. J. Biol. Macromol. 243, 125219.

Zhou, N., Thilakarathna, W.P.D.W., He, Q.S., Rupasinghe, H.P.V., 2022. A Review: Depolymerization of Lignin to Generate High-Value Bio-Products: Opportunities, Challenges, and Prospects. Front. Energy Res. 9, 758744.